Fingerprint Matching using Enhanced Shape Context

Paul W.H. Kwan[1], Junbin Gao[2], and Yi Guo[1]

[1] School of Mathematics, Statistics and Computer Science, University of New England, Armidale NSW 2351, Australia.

[2] School of Information Technology, Charles Sturt University, Bathurst NSW 2795, Australia.

Email: {kwan, yguo4}@mcs.une.edu.au, jbgao@csu.edu.au

Abstract

Shape context, a robust descriptor for point pattern matching, is applied in fingerprint matching by enhancing with minutiae type and angle details. A modified matching cost between shape contexts, by including the application specific contextual information, improves the accuracy of matching when compared with the original definition. To reduce computation for practical use, a simple pre-processing step termed elliptical region filtering is applied in removing spurious minutiae prior to matching. Empirical experiments conducted on a database of fingerprint images confirmed the improvements in accuracy and speed attained by the proposed method.

Keywords: fingerprint matching, minutiae, shape context, elliptical region filtering, point pattern matching

1 Introduction

Biometric recognition is a technology for confirming a person's identity based on his physiological and behavioural traits. Among these, fingerprints, face, speech, iris and hand geometry are most commonly used [1]. An early application of this technology was Automatic Fingerprint Identification System (AFIS) found in law enforcement. Recently, a number of non-forensic applications like secured access to restricted areas, network login, etc appeared.

Post-evaluation of the terrorist attacks that occurred in America on September 11, 2001 called for increase in surveillance both within the country and at border control. Primary activities are identity verification and matching against a list of suspects. To automate these activities, America and her partners in the visa-waiver program developed their biometric passports based on standards defined by the International Civil Aviation Organisation (ICAO). Currently, digital images of fingerprints, face, or iris are stored only. The main performance requirements are accuracy and speed.

This work attempts to address both the accuracy and speed in automatic fingerprint identification. The method proposed belongs to the class of minutiae-based fingerprint matching [1]. Like most methods in this class, the presence of spurious minutiae adversely affects the accuracy. In addition, the computational overhead could increase considerably, rendering the method impractical for online application.

In practice, one can model minutiae matching as a kind of point pattern matching. Recently, a robust descriptor called shape context was proposed and its effectiveness demonstrated in general shape matching involving point patterns [2]. In the original paper, application-specific contextual information was not considered. The sets of points on both shapes were randomly selected. However, as the authors pointed out, application-specific contextual information can be exploited to improve accuracy. This is one of the major motivations underpinning this work.

In this paper, our contributions are two-fold. First, a simple pre-processing method called *elliptical region filtering* is proposed to filter out potential spurious minutiae that were introduced in preliminary minutiae extraction. To assess its effectiveness, two simple metrics motivated by the precision and recall adopted in information retrieval research are defined and verified by experiments.

Second, by including minutiae type and angle details as application-specific contextual information, we are able to improve the matching accuracy versus speed ratio over the original shape context in cases where large number of minutiae were removed by filtering.

The rest of the paper is organized as follows. Section 2 briefly reviews related work. Section 3 explains our method in detail, supported by empirical experimental results. Section 4 concludes with future directions.

2 Related Work

Fingerprint matching methods can be largely grouped into three main classes, including correlation-based matching, ridge feature-based matching, and minutiae based matching [1]. In correlation-based matching, correlation between corresponding pixels on a pair of fingerprint images is computed for various alignments like displacement and rotation and used for matching. In ridge feature-based matching, features like local orientation, frequency and shape of ridge patterns are

used. In minutiae based matching, minutiae are first extracted from the fingerprint images and stored as sets of points on a two-dimensional plane. Matching essentially consists of finding the alignment between the template and the input minutiae sets that result in the maximum number of pairings. Fig. 1 shows a fingerprint with two kinds of minutiae marked.

The process of finding an optimal alignment between the template and the input minutiae sets can be modelled as point pattern matching. Recently, the shape context, a robust descriptor for point pattern matching was proposed in the literature. According to experiments on the MNIST handwritten digit database and the MPEG-7 shape silhouette database, the shape context was reported to outperform a number of well-known methods [2]. However, in the original definition, it only considered the distribution of the remaining points with respect to each selected point. While the authors mentioned the possibility of including application specific contextual information in the definition, no concrete suggestion was given. In this work, both minutiae type and angle details are applied as application specific contextual information to enhance the original shape context, leading to improved matching accuracy.

A major problem that could degrade the accuracy of minutiae-based matching is due to spurious minutiae extracted from poor quality fingerprint images. These could result from dry skin, a person's age or his occupation. Pre-processing steps utilizing fingerprint enhancement and minutiae filtering algorithms have been reported in the literature [3, 1]. In this work, a method similar to Hong et al. [3] was applied in fingerprint enhancement, while a method called elliptical region filtering is proposed to remove potential spurious minutiae. Spurious minutiae often occur along the edge between areas of a fingerprint that either touch or not touch the scanner surface.

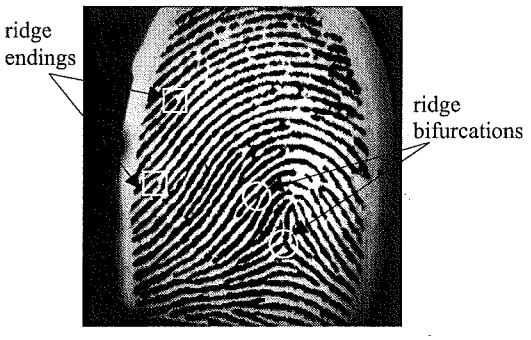

Figure 1: Fingerprint with minutiae marked.

3 Proposed Method

Existing minutiae-based matching methods largely comprises the following four processing stages:

- *Fingerprint enhancement*: features in poor quality fingerprint image are enhanced before extraction.
- *Minutiae extraction*: in most cases, ridge endings and ridge bifurcations are detected and extracted from the enhanced image.
- *Minutiae filtering*: an optional stage in which spurious minutiae that can degrade both accuracy and speed of matching are filtered.
- *Fingerprint matching*: two sets of minutiae, one for the input and another for the template, are matched. A score that measures their similarity (or dissimilarity) is computed and compared to a threshold to decide either acceptance or rejection.

Here, our contributions lie in the stages of minutiae filtering and fingerprint matching. For completeness sake, we will describe briefly fingerprint enhancement and minutiae extraction as used in this work.

Fingerprint enhancement follows largely the approach reported in Hong et al. [3]. First, ridge regions in the input image are identified and normalised. Next, the ridge orientations are determined. Third, local ridge frequencies are calculated. Fourth, contextual filters with the appropriate orientations and frequencies are applied. Fifth, binarization is performed resulting in a black and white image of the fingerprint. Fig. 2's upper half presents the output of the steps in the enhancement process.

Minutiae extraction starts by thinning the black and white fingerprint image resulted from enhancement. From the thinned image, potential minutiae are detected and extracted by tracking the set of one pixel width edges. Fig. 2's lower half shows both the thinned image and the minutiae extracted, with 'o' indicates ending and '+' a bifurcation.

3.1 Minutiae Filtering

In this work, a simple method called *elliptical region filtering* is proposed to remove potential spurious minutiae in order that the computational overhead in matching a pair of fingerprints can be reduced while accuracy could be maintained. This method is motivated by the observation that the surface of a fingerprint that touches the sensor can be modelled as an ellipse (Refer to the filtered image in Fig. 2 for the idea). As a result, true minutiae are more likely extracted within the ellipse than would be on or outside the boundary (Refer to the bottom left image in Figure 2 for the argument).

As mentioned, the method we proposed makes use of a simple geometric property of an ellipse. In the ellipse shown in Fig. 3, the centre is M while both F1 and F2 are the foci that lie on its major axis. The length of the major axis is $a/2$, while that of minor axis is $b/2$. For any point P, one way to determine if it is inside an ellipse is by using the following formula:

$$\frac{x^2}{a^2}+\frac{y^2}{b^2} < 1 \qquad (1)$$

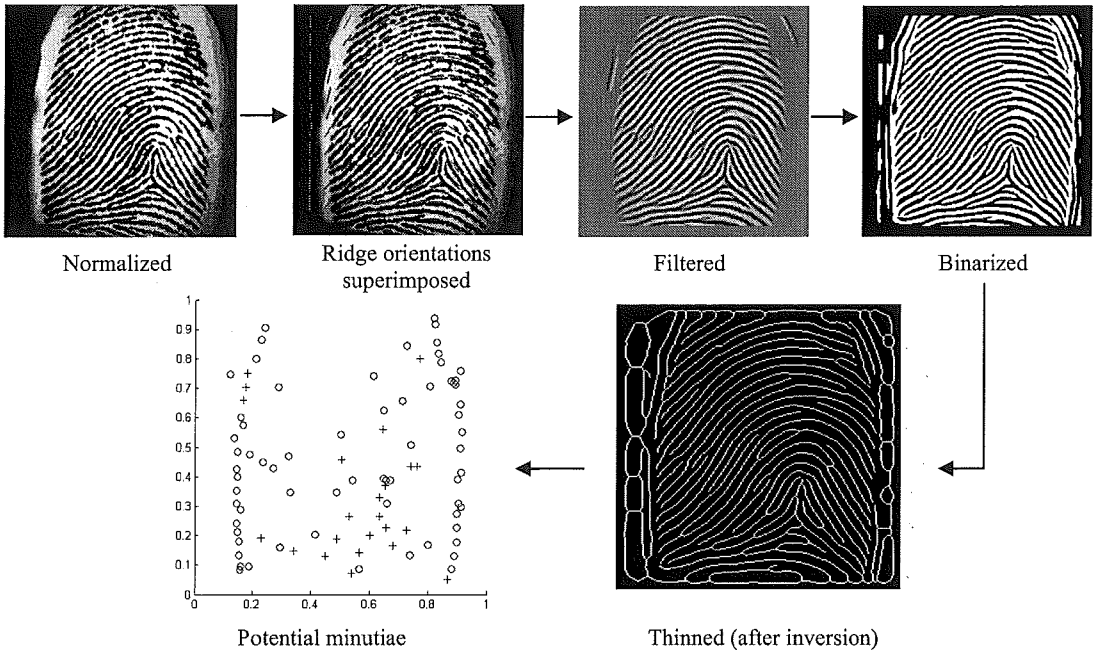

Figure 2: Fingerprint enhancement and Minutiae extraction

where (x,y) are coordinates of P on a plane. Here, our objective is to remove minutiae that lie outside of the ellipse. That is, we want to retain points like *P1* but not *P2* or *P3*. To compute this efficiently, we make use of another definition of ellipse that the circumference is the set of points such that the sum of the distances from each point to the two foci equals $2a$, which is the length of the major axis. In other words, a point is inside an ellipse if the sum of the distances is less than $2a$.

Formally, if we denote the two foci vectors that point from M to F1 and M to F2 by *C1* and *C2* respectively, a point P is inside the ellipse when

$$|P-C1|+|P-C2| \;<\; 2a \qquad (2)$$

Using this idea, filtering minutiae is carried out as follow. First, we compute the smallest *rectangular bounding box* that encloses all the minutiae. Taking the longer side of the box as the length of the major axis of an ellipse, we fit it inside the bounding box. By referring to equation (2), we determine if each of the minutiae falls inside the ellipse or not. Those that are not will be filtered.

Fig. 4 shows the sets of minutiae extracted both before and after applying elliptical region filtering. The one on the left plot is the pre-filtered set and has 90 minutiae altogether, while the one on the right plot has 53 minutiae, just several more than half the size of the pre-filtered set. By comparing the before and after images, we can verify that most of the false endings due to the boundary effect have been filtered, while those that lie within the centred or "confident" region remained.

We understand that this simple filtering procedure can potentially remove genuine minutiae as neither the structural nor the contextual information of each minutia was examined. To evaluate its effectiveness empirically, we define two simple metrics based on the *precision* and *recall* that are used in Information Retrieval research as follows:

$$precision = \frac{\#\ genuine\ \ minutiae}{\#\ extracted\ \ minutiae} \qquad (3)$$

$$recall = \frac{\#\ genuine\ \ minutiae}{\#\ ground\ \ truth\ \ minutiae} \qquad (4)$$

Here, the set of genuine minutiae is the subset of the total extracted minutiae that are in the set of *ground truth* minutiae. By ground truth minutiae, we are referring to those that are agreed visually by 2 out of 3 human subjects. Using the same fingerprint shown in Fig. 1 and Fig. 2 as example, the number of ground truth minutiae is 37. Out of 90 minutiae in the pre-filtering set, 33 are genuine minutiae. Compared to this, out of 53 minutiae in the post-filtering set, 32 are genuine minutiae.

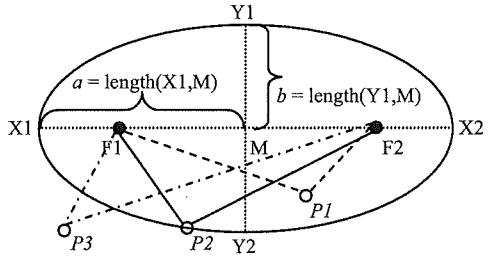

Figure 3: An ellipse showing the centre and foci

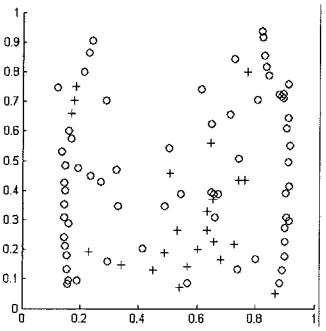

Pre-filtering minutiae set

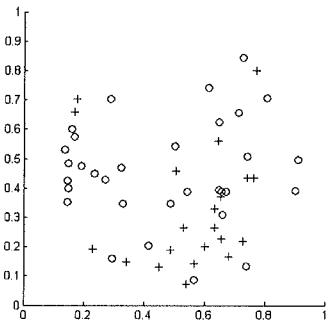

Post-filtering minutiae set

Figure 4: The sets of minutiae both before (90) and after (53) applying elliptical region filtering

Based on equations (3) and (4), the values for *precision* and *recall* are 0.36 and 0.89 for pre-filtering, while those for post-filtering are 0.60 and 0.86. By comparing these figures, we notice that *precision* in fact improves in the post-filtering set while *recall* is largely maintained. Comparable figures were obtained in our extensive experiments involving other fingerprint images in the database. Based on these empirical results, the following two conclusions can be drawn. First, the proposed filtering method does not adversely affect the set of genuine minutiae extracted. Second, both the total number and the number of false minutiae (factors that might decrease matching accuracy while increasing computational load) are largely reduced.

3.2 Fingerprint Matching

In this section, we will explain how the shape context proposed recently in [2] is enhanced and applied in matching a pair of fingerprints whose minutiae are modelled as point patterns. To provide the necessary background for our explanation, we briefly summarize below how the shape context is constructed for the set of filtered minutiae of a fingerprint shown in Fig. 5. They will be used in matching the minutiae of the fingerprint shown in right hand plot of Fig. 4 in our discussion.

Basically, there are four major steps in the shape context based fingerprint matching (Fig. 6):

- *Construct shape context*: for every minutia p_i, a coarse histogram h_i of the relative coordinates of the remaining $n-1$ minutiae is computed,

$$h_i(k) = \#\{q \neq p_i : (q - p_i) \in bin(k)\}. \quad (5)$$

The bins are uniform in the log-polar space (Fig. 5). To measure the cost of matching two minutiae, one on each of the fingerprints, the following formula based on the χ^2 test statistic:

$$C_{ij} \equiv C(p_i, q_j) = \frac{1}{2}\sum_{k=1}^{K}\frac{[h_i(k) - h_j(k)]^2}{h_i(k) + h_j(k)}. \quad (6)$$

The set of all costs C_{ij} for all pairs of minutiae p_i on the first and q_j on the second fingerprint are similarly computed.

- *Minimize matching cost*: given all costs C_{ij} in the "current" iteration, this step attempts to minimize the total matching cost,

$$H(\pi) = \sum_i C(p_i, q_{\pi(i)}). \quad (7)$$

Here, π is a permutation enforcing a one-to-one correspondence between minutiae on the two fingerprints. (Top right hand plot of Fig. 6 illustrates the set of initial correspondences)

- *Warping by TPS transformation*: given the set of minutiae correspondences, this step tries to estimate a modelling transformation T: $R^2 \rightarrow R^2$ using thin plate spline (TPS) to warp one onto the other. The objective is to minimize bending energy of the TPS interpolation by $f(x,y)$ as,

$$I_f = \iint_{R^2}\left(\frac{\partial^2 f}{\partial x^2}\right)^2 + 2\left(\frac{\partial^2 f}{\partial x \partial y}\right)^2 + \left(\frac{\partial^2 f}{\partial y^2}\right)^2 dxdy \quad (8)$$

Further details on the form of the interpolant $f(x,y)$ and the interpolation conditions can be found in [2].

This and the previous two steps are repeated for several iterations (5 in our experiments) before the final distance that measures the dissimilarity of the pair of fingerprints is computed. (Refer to the two bottom plots of Fig. 6 for the idea)

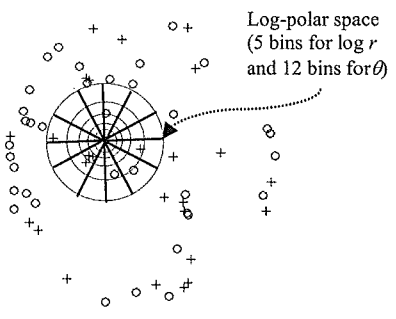

Figure 5: Shape context of a fingerprint's minutia

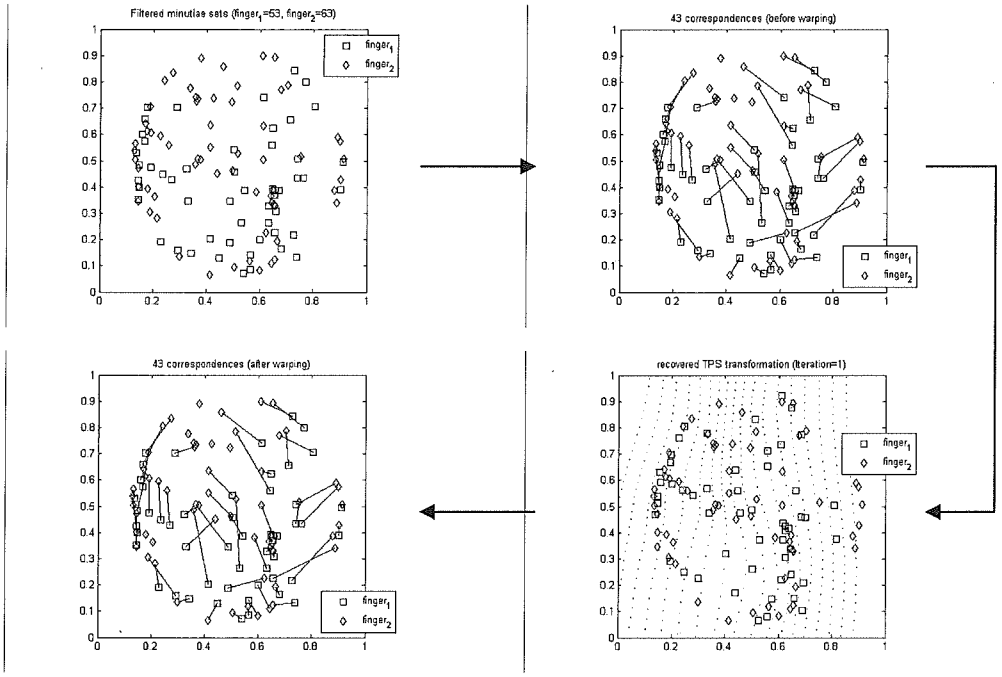

Figure 6: Major steps in shape context based fingerprint matching

- *Calculate final distance*: in the original paper, the final distance D is defined as,

$$D = D_{sc} + \alpha D_{ac} + \beta D_{be}. \quad (9)$$

where D_{sc} is the shape context cost calculated after the iterations, D_{ac} an appearance cost, and D_{be} the bending energy. Both α and β are constants determined by experiments. In this work, D_{ac} is not included as it is relevant only for grayscale images while the image here is binary. The distance D is thus defined as,

$$D = D_{sc} + \beta D_{be}. \quad (10)$$

By repeated experiments using our database, the optimal value for $\beta \in [0,1]$ is found to be 0.1. For each fingerprint in the database, its distance from the input is calculated. A final ranking in which the top has the least distance from the input is obtained.

3.2.1 Enhanced Shape Context

Initially, we applied shape context without filtering. The database we used contains 21 different fingers, each having 8 impressions totalling 168 fingerprint images. For our notation, 1_1 denotes the first impression of finger 1 while 21_8 the eighth of finger 21. Although the size of our database might be small, it is adequate for illustrating our idea.

Even in the presence of a larger number of spurious minutiae, matching by the original shape context is still quite effective (Refer to the two pre-filtered ranking columns in Table 1). For example, when input fingerprint is 1_1, all remaining 7 impressions plus itself came in the top 8 of the final ranking. For fingerprint 2_1, though the result is not as spectacular as 1_1, 6 out of 8 impressions came in the top 9 ranking. This speaks strongly the intrinsic robustness of the shape context matching model.

But, the practical problem we face is speed. Even though CPU time cannot be considered an accurate estimate of computational load, it could provide an idea on how efficient fingerprint matching with the original shape context runs. In the case of matching 1_1 and 2_1 against the database, the times are 697 sec and 850 sec, limiting its usefulness in practice.

Table 1: Matching results by original shape context

 1_1			 2_1		
	pre-filtered ranking	post-filtered ranking		pre-filtered ranking	post-filtered ranking
1_1	1	1	2_1	1	1
1_2	4	3	2_2	29	57
1_3	6	6	2_3	9	4
1_4	2	2	2_4	3	41
1_5	7	84	2_5	2	2
1_6	3	4	2_6	100	61
1_7	5	5	2_7	7	129
1_8	8	45	2_8	5	75

To reduce execution time, we apply filtering before matching. The matching times become 120 sec and 161 sec, which are less than 20% the pre-filtered figures. However, accuracy is degraded when we compare the rankings in the post-filtered columns with those of the pre-filtered columns in Table 1. The goal of improving the matching accuracy while maintaining the reduction in execution time leads to *enhanced shape context* that is described below.

In our formulation, minutiae type and angle details are incorporated as application-specific contextual information to enhance the original shape context. To accomplish that, we define a new matching cost C_{ij}^* between two minutiae p_i and q_j as,

$$C_{ij}^* \equiv C^*(p_i, q_j) = \left(1 - \gamma C_{ij}^{type} C_{ij}^{angle}\right) C_{ij} \qquad (11)$$

Here, C_{ij} is the original shape context cost defined in equation (6), C_{ij}^{type} the cost in matching the type of p_i and q_j, C_{ij}^{angle} the cost in matching the ridge orientations tangent at p_i and q_j respectively, and $\gamma \in [0,1]$ whose optimal value is tuned by repeated experiments. Note that the multiplications between C_{ij}^{type}, C_{ij}^{angle} and C_{ij} in equation (11) are scalar (i.e., element-by-element) rather than the usual matrix multiplication. C_{ij}^{type} and C_{ij}^{angle} are defined as,

$$C^{type}(p_i, q_j) = \begin{cases} -1, & type(p_i) = type(q_j) \\ 0, & type(p_i) \neq type(q_j) \end{cases} \qquad (12)$$

where the *type* is either ridge ending or bifurcation.

$$C^{angle}(p_i, q_j) = -0.5 * \left(1 - \cos\left(\angle_{initial-warped}\right)\right) \qquad (13)$$

where $\angle_{initial-warped}$ is the absolute value of the difference in ridge orientations tangent at p_i and q_j in the beginning and after each iterative warping. If $\angle_{initial-warped}$ is greater than π, it is adjusted as $(2\pi - \angle_{initial-warped})$ so it will be less than or equal to π.

Table 2: Compare matching results by original and enhanced shape contexts

	 1_1			 2_1	
	original shape context	enhanced shape context		original shape context	enhanced shape context
1_1	1	1	2_1	1	1
1_2	3	3	2_2	57	37
1_3	6	6	2_3	4	53
1_4	2	2	2_4	41	3
1_5	84	48	2_5	2	2
1_6	4	4	2_6	61	38
1_7	5	5	2_7	129	123
1_8	45	41	2_8	75	15

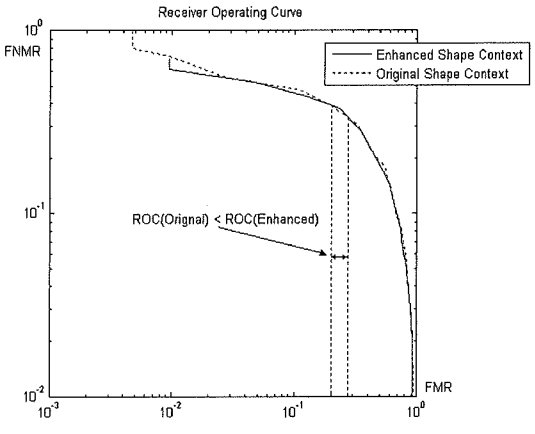

Figure 7: Compare ROCs between the enhanced and original shape contexts

In Table 2 the enhanced shape context is compared with the original after filtering is applied. For 1_1, it is clear that the enhanced shape context improves the rankings of both 1_5 and 1_8 while the other six remain same. For 2_1, most rankings improve except for 2_3. But, it is able to preserve the top 3 entries of the pre-filtered column in Table 1, which is not possible with the original shape context.

Next, in Figure 7, we compare them over the entire database by the ROCs (Receiver Operating Curves) constructed using the FMR (False Match Rate) and the FNMR (False Non-Match Rate). These figures are computed from 588 genuine and 210 imposter matching attempts as in [1]. Other than the small range indicated in the figure, the ROC of enhanced shape context consistently achieves a slightly lower or equal joint FMR and FNMR than the original.

4 Conclusions

In this paper, the shape context descriptor is applied in fingerprint matching by enhancing with minutiae type and angle details. The modified shape context cost improves matching accuracy when compared to the original definition. To reduce computation, elliptical region filtering is proposed for removing spurious minutiae prior to matching. Experiments confirmed the improvements in accuracy and speed attained by the proposed method.

5 References

[1] D. Maltoni, D. Maio, A. Jain, and S. Prabhakar, *Handbook of Fingerprint Recognition*: Springer, 2003.

[2] S. Belongie, J. Malik, and J. Puzicha, "Shape Matching and Object Recognition Using Shape Context," *IEEE Trans. PAMI,* vol. 24, no. 24, pp. 509–522, 2002.

[3] L.Hong, Y. Wan, and A. Jain, "Fingerprint Image Enhancement: Algorithm and Performance Evaluation," *IEEE Trans. PAMI,* vol. 20, no. 8, pp. 777–789, 1998.